Nitrogen Doped Graphene Nanoribbons for Organic Photovoltaic Applications

Donatela Bellone
Ana Claudia Arias

Electrical Engineering and Computer Sciences
University of California at Berkeley

Technical Report No. UCB/EECS-2016-186
http://www2.eecs.berkeley.edu/Pubs/TechRpts/2016/EECS-2016-186.html

December 1, 2016

Nitrogen Doped Graphene Nanoribbons for Organic Photovoltaic Applications

By

Donatela Elsa Bellone

A report submitted in partial satisfaction of the

requirements for the degree of

Master of Science

in

Electrical Engineering and Computer Science

in the

Graduate Division

of the

University of California, Berkeley

Committee in charge:

Professor Ana Claudia Arias, Advisor
Professor Constance Chang-Hasnain, Second Reader

Spring 2016

Nitrogen Doped Graphene Nanoribbons for Organic Photovoltaic Applications

Abstract

Nitrogen Doped Graphene Nanoribbons for Organic Photovoltaic Applications

by

Donatela Elsa Bellone

Master of Science in Electrical Engineering and Computer Science

University of California, Berkeley

Professor Ana Claudia Arias, Advisor

Fabrication of organic photovoltaic devices employing nitrogen-doped graphene nanoribbons is reported herein. Graphene nanoribbons are of interest to organic photovoltaic devices due to their high mobility, high thermal and atmospheric stability, and tensile strength. In this study, we observed that inclusion of graphene nanoribbons as electron acceptors in a P3HT polymer cell decreases the series resistance by providing conductive pathways. Additionally, optical studies confirm an increase in the order of the film by addition of graphene nanoribbons (GNR). The devices containing GNRs have superior performance to those of pristine P3HT. A V_{oc} of 0.51 V, J_{sc} of -4.07 x 10^{-5} A/cm^2, power conversion efficiency (PCE) of 0.00643, and fill factor of 0.31 was obtained by fabricating a device from P3HT/GNR solutions aged overnight with cyclohexanone. Polymers cells using PCDTBT as a donor and $PC_{71}BM$ as the acceptor were also studied due to the polymer's significantly different morphology to P3HT. The addition of 2% of graphene nanoribbons provides a conductive pathways for electrons to reach the cathode, an effect observed in the decrease in series resistance, improvement of J_{sc} of 15%, and an increase in PCE of 18%. The figures of merit for this cell were Voc = 0.92 V, Jsc = -7.34 x 10^{-3} A/cm^2, PCE of 3.41%, and a fill factor of 0.5. To our knowledge this is the first study employing atomically defined graphene nanoribbons in organic photovoltaics, showing promise of the material as current and efficiency enhancers.

To Logan,

who knows how to make me smile with his gentle paw,

and

To Zach,

husband and Logan's dad,

for being supportive in the sweetest ways possible

Table of contents

Acknowledgments

The role of graduate school is to train the next generation of thinkers and researchers by inspiring their creativity, supporting their endeavors, and guiding them in moments of need. It is not always easy to be a good mentor. Professor Ana Claudia Arias has the right recipe to balance support and expectations, and helping her students succeed and ripe in a good team environment. I would like to thank her above every one else for allowing me to conduct research in her lab, guiding me through the process of entering a new field, and having no judgment whenever I encountered a block. She has been mentoring me as an outside member for my chemistry dissertation, and I am lucky to be given the opportunity to get to know her better.

Secondly, I am thankful to Professor Constance Chang-Hasnain for kindly agreeing to be my second reader. I met Professor Chang-Hasnain back in 2015 when I took her class in Nanoscale Fabrication. Her class ignited in me a curiosity for the field of nanotechnology and its potential applications.

Next, this work wouldn't have been possible without the support of my chemistry PhD advisor, Professor Felix Raoul Fischer. It is not common for an untenured professor to allow his students full reign in their graduate school career. He supported my transition the electrical engineering department and remains active with feedback for research being carried out outside of his lab.

Additionally, I would like to thank the Arias group. In particular, I am thankful to Claire Lochner and Jonathan K'ang-Yu Ting, who taught me everything about device fabrication, from spin-coating to evaporation; Balthazar Lechêne who taught me about the little tricks of device fabrication and troubleshooting results; Igal Deckman for his helpful advice and always honest feedback; Adrien Pierre and Alla Zamarayeva for conducting experiments I was not familiar with; and Aminy Ostfield for proofreading this report and explaining the fundamentals of organic photovoltaics. Most importantly, I am appreciative of the Arias group as a whole for making me feel welcomed from day one.

Finally, like to so many people, I wouldn't be where I am without the ongoing support of my family: my parents who made the sacrifice of leaving their home country to give me a better future; and my sister for being a warrior in life and a source of inspiration. Their encouragement and ongoing understanding is present whenever I need it. Your belief in me is all I need.

1 Introduction

1.1 Organic Photovoltaics

Organic photovoltaics (OPVs) describe a group of solar cells where the photo-active layer consists of hydrocarbon-based materials, usually polymer donor and fullerene acceptors. These devices provide an attractive, scalable way to obtain clean, renewable energy, and are of interest to niche markets including flexible electronics or building energy integration.[1] OPVs may be cheaply and efficiently printed on flexible substrates, allowing for roll-to-roll processing compatible with large-scale industrial fabrication.[2] Recently, thin film organic photovoltaics with efficiencies as high as 11.0% have been reported, emphasizing the potential application of these materials.[3] The increase in efficiency of OPVs since their discovery has mostly been due to the discovery of new OPV materials and the optimization of such.[4] However, much improvement is necessary in order to achieve the Shockley-Quessier limit of 33% predicted for a single p-n junction solar cell at the ambient temperature with a 1.4 eV band gap.[5] Additionally, OPVs do not have a long lifetime, and remain far behind the most common silicon technologies, which have reached efficiencies of 27.6% as shown in the NREL chart shown below (Figure 1).

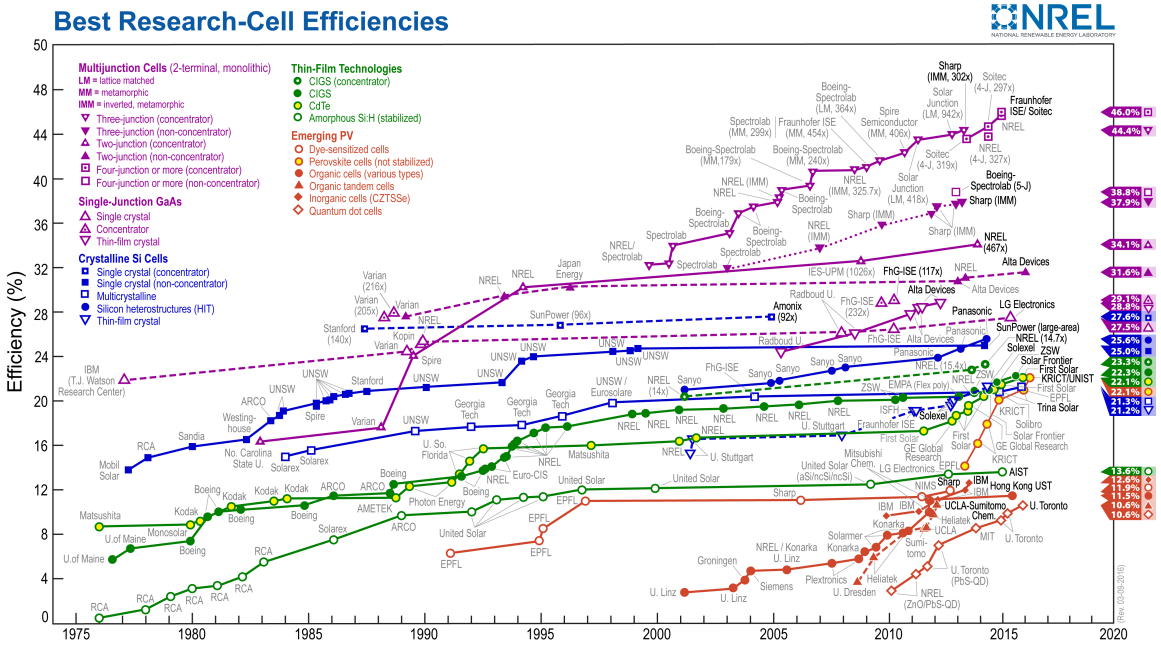

Figure 1. Solar cell efficiency records obtained from NREL.

The method of current generation in OPVs is analogous to that of a p-n junction solar cell, yet different. Unlike their inorganic counterparts, OPVs have a much lower dielectric constant which results in minimal screening of the columbic attraction between holes and electrons.[6] Upon light absorption, an exciton is formed rather than free carriers. In order for this exciton to generate current, it must become a hole and an electron. If this doesn't occur within the lifetime of the exciton, it may decay back to its ground state, resulting in the loss of energy as light or thermal energy. Usually, a donor/acceptor blend similar to the p-n junction allows for the separation of free charges as long as the difference between the lowest unoccupied molecular orbital (LUMO) of the donor and the acceptor is greater than the binding energy of the exciton. Once the electron is transferred to the acceptor, the charge transfer complex is created. The carriers must diffuse beyond the coulomb capture radius to avoid recombination at the donor/acceptor

interface. Each respective free carrier may then travel to the cathode or anode, as long as no trap states result in charge recombination.

The formation of free carriers upon illumination results in current and voltage generation. Under short circuit situations, the current flow (J_{sc}) is at a maximum. In order to obtain high current, absorption of photons must be high and recombination minimal. The maximum electrochemical potential for the OPV (V_{oc}) occurs with no current flow. To a first approximation, the open circuit voltage may be determined by the difference between the highest occupied molecular orbital (HOMO) of the donor and the LUMO of the acceptor. The fill factor (FF) is the ratio of the current and voltage at maximum power to the J_{sc} and V_{oc}. The FF is a measure of ideality of the solar cell, and it should be 1. Additionally, another important figure of merit is the power conversion efficiency (PCE). The PCE may be calculated by the ratio of the multiplication of the fill factor, the open circuit voltage, and the short circuit voltage, to the input power. Ongoing efforts are being done on the optimization of known solar cell architectures and materials, as well as the discovery of novel OPV components.

Factors limiting the efficiency of current organic solar cells include morphological instability of conducting polymers, recombination of electron-hole pairs, degradation of the polymer, trap defects, and other inefficiencies in light absorption, exciton diffusion, exciton dissociation, charge transport, and charge collection.[2,4,7,8] Most of the research of OPV optimization utilizes fullerene derivatives as acceptors, such as [6,6]-phenyl-C61-butyric acid methyl ester (PCBM). Although relative high efficiencies are achieved with this material, PCBM and analogous fullerenes remain one of the most expensive portions of an OPV, while also affecting current generation by decreasing the absorption of the

cell at high PCBM concentrations. Moreover, recent studies have shown that PCBM molecules tend to aggregate at the bottom during spin coating of the donor/acceptor blend.[9] This phase segregation highly impacts the efficiency of the solar cell. In particular, it deters the efficiency of the most common architecture and improves that of inverted structures. Finally, the small volume of PCBM, makes the acceptor far from ideal for carrier transport, such that the electrons are required to travel through various PCBM molecules before reaching the cathode.

Therefore, it would be ideal to use an anisotropic acceptor with similar dispersion properties as the donor polymer. Increasing the mobility of the charge carriers as well as decreasing defects within the materials themselves would reduce the chance of recombination events and, thus, increase the current and efficiency of the cell.[2,8,10]

1.2 Graphitic Material in Organic Photovoltaics

In recent years, graphitic structures such as reduced graphene oxide and carbon nanotubes have been studied as transport layers, transparent electrodes, and acceptor materials in OPVs.[11] Graphitic materials may be easily tunable by doping, width variation, and defect incorporation, making them versatile components of OPVs. Additionally, they are of interest due to their thermal stability, high mobility, stiffness, solvent resistance, optical anisotropy, and ability to increase the glass transition temperature of the cell.[11,12]

More than a decade ago, Kymakis et al. reported the first use of carbon nanotubes (CNT) as the electron acceptor material in an OPV.[13] Single-wall carbon nanotubes dispersed within a film of *poly*(3-hexylthiophene-2,5-diyl) (P3HT) provided percolation paths for electrons, leading to a tenfold increase in conductivity compared to the pristine

polymer cells. They achieved a high V_{oc} of 0.75 V compared to typical P3HT cells (0.35 V), yet had a small PCE of 0.04% due to inefficient charge transfer (PCE = 2.5 x 10^5 for pristine devices). Similarly, solution-processable functionalized graphene as the electron acceptor in a P3HT solar cell was described by Liu et al., obtaining power conversion efficiencies of up to 1.4%.[14,15] Surprisingly, defect filled 2D graphene and reduced graphene oxide typically result in solar cells with better performance than carbon nanotubes, due to their capability of intercalating within the polymer matrix, their dispersibility in solvents, and their flexibility resulting in stronger π-π interactions.[16] Perhaps the most notable attribute to this class of materials would be as performance enhancers by providing pathways for transport. Berson et al. reported a 225% increase in PCE and a 50% increase in J_{sc} by including 0.1 wt% of multi walled carbon nanotubes in a P3HT/PCBM solar cell.[17] As shown in Figure 2, the multi-walled nanotubes (MWNT) acts as a hole transport pathway to the anode. Low efficiencies of graphitic materials based OPVs can be associated with reducing the shunt resistance, impurities, aggregation, and low charge carrier mobility within the matrix.

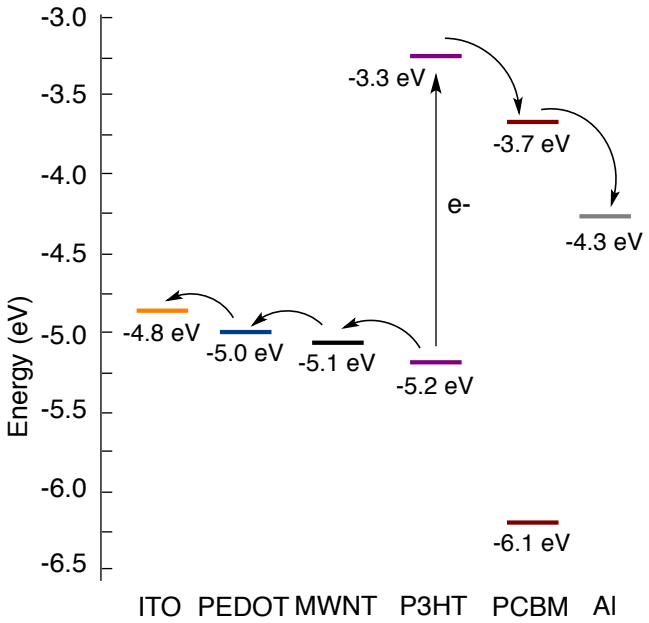

Figure 2. Energy levels of the single components of the photovoltaic cell ITO/PEDOT/P3HT/CNT:PCBM/Al device with CNTs.[17]

1.3 Graphene Nanoribbons in Organic Photovoltaics

Graphene is a 2D sheet of sp^2 carbon, where free charges are capable of moving outside of the plane of the atoms. Graphene has metallic properties and a band gap of 0. However, 1D graphene, also known as graphene nanoribbons (GNR) have a finite band gap while maintaining the transport properties of graphene. Graphene nanoribbons have recently caught the attention of the scientific community for their notable properties. GNRs are of interest to OPVs due to their inertness to ambient conditions, high charge carrier mobility, direct band gap, high absorbance, high thermal conductivity, and tensile strength.[18] By controlling the edge structure of the GNRs, the edge defects that increase the probability of recombination can be eliminated. Unlike carbon nanotubes or graphene, the dispensability, band gap, and the energies of the HOMO/LUMO may be tuned by

controlling the edge of the GNR through a bottom up synthesis. In this procedure, a monomer is designed with the desired characteristic of the final GNR in mind, avoiding post-polymerization procedures that lead to defects, such as the common oxidation/functionalization reactions of GNT and graphene.

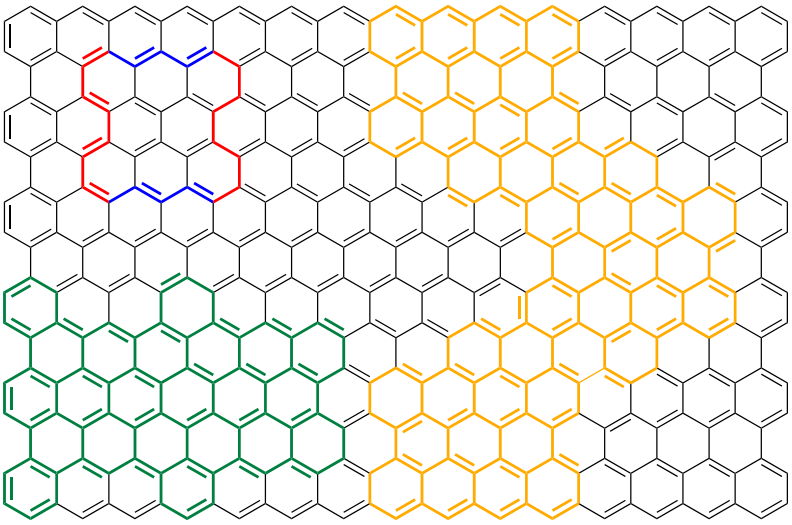

Figure 3. Depiction of zigzag (blue), armchair (red), chevron (yellow), and cove (green) GNRs.

GNRs provide the middle ground between CNT and graphene sheets. They are anisotropic, highly conductive, and tunable, yet they are flexible, defect-free functionalizable, and possess a high surface area which provides the right morphological architecture for exciton dissociation. Edge structure defines the conductivity of GNRs, with zigzag GNRs being metallic (blue in Figure 3) and armchair GNRs being semiconducting (red in Figure 3). Two common GNRs synthesized in solution are chevron (yellow in Figure 3) and cove-type (green in Figure 3). Finally, the band gap of semiconducting armchair GNRs may be tuned by changing the width of the ribbons. Similarly, the position of the HOMO/LUMO bands may be shifted by the right choice of dopant.

Graphene nanoribbons have only recently been synthesized in solution. Their use in organic photovoltaics remains scarce. In 2015, Lee et al. reported the use of graphene nanoribbons as hole transport layer in an OPV containing poly[[4,8-bis[(2-ethylhexyl)oxy]benzo-[1,2-b:4,5-b0]dithiophene-2,6-diyl][3-fluoro-2-[(2-ethylhexyl)carbonyl]-thieno[3,4-b]thiophenediyl]]:6,6-phenyl-C71-butyric acid methyl ester (PTB7:$PC_{71}BM$) as the active layer.[19] They observed a PCE of 7.6% from an inkjet printed OPV compared to a similar device fabricated with PEDOT:PSS as the hole transport layer (PCE = 7.32%). To our knowledge, this is the only report of employing GNRs in polymer solar cells. The lack of commercially available graphene nanoribbons and the difficulty of synthesis of defect free materials could possibly be main reason why GNRs have not been widely implemented in the field of OPVs. Herein, we report initial attempts at using nitrogen-doped GNRs as electron acceptors and as electron transport pathways in OPVs.

1.4 Structure of the dissertation

There are four chapters in this technical report. Chapter 2 consists of the synthesis and characterization of nitrogen doped graphene nanoribbons. Their application in OPVs as electron acceptors and electron transport pathway in P3HT solar cells is discussed in Chapter 3. Their application as solar cell additives with *poly*[*N*-9′-heptadecanyl-2,7-carbazole-*alt*-5,5-(4′,7′-di-2-thienyl-2′,1′,3′-benzothiadiazole)], Poly[[9-(1-octylnonyl)-9H-carbazole-2,7-diyl]-2,5-thiophenediyl-2,1,3-benzothiadiazole-4,7-diyl-2,5-thiophenediyl] (PCDTBT) as the donor is investigated in Chapter 4.

1.5 References

(1) Nielsen, T. D.; Cruickshank, C.; Foged, S.; Thorsen, J. *Solar Energy Materials ...* **2010**, *94* (10), 1553.

(2) Kippelen, B.; Brédas, J.-L. *Energy & Environmental Science* **2009**, *2* (3), 251.

(3) Green, M. A.; Emery, K.; Hishikawa, Y. *Progress in ...* **2015**.

(4) DeLongchamp, D. M. In *Semiconductor Materials for Solar Photovoltaic Cells*; Springer Series in Materials Science; Springer International Publishing: Cham, 2016; Vol. 218, pp 169–196.

(5) Shockley, W.; Queisser, H. J. *Journal of Applied Physics* **1961**, *32* (3), 510.

(6) Mazzio, K. A.; Luscombe, C. K. *Chem. Soc. Rev.* **2015**, *44* (1), 78.

(7) Jackson, N. E.; Savoie, B. M.; Marks, T. J.; Chen, L. X.; Ratner, M. A. *J. Phys. Chem. Lett.* **2015**, *6* (1), 77.

(8) Janssen, R. A. J.; Nelson, J. *Adv. Mater.* **2012**, *25* (13), 1847.

(9) Xu, Z.; Chen, L. M.; Yang, G.; Huang, C. H.; Hou, J.; Wu, Y.; Li, G.; Hsu, C. S.; Yang, Y. *Adv. Funct. Mater.* **2009**, *19* (8), 1227.

(10) Su, Y.-W.; Lan, S.-C.; Wei, K.-H. *Materials Today* **2012**, *15* (12), 554.

(11) Ratier, B.; Nunzi, J. M.; Aldissi, M.; Kraft, T. M. *Polymer* **2012**.

(12) Ramanathan, T.; Abdala, A. A.; Stankovich, S.; Dikin, D. A.; Herrera-Alonso, M.; Piner, R. D.; Adamson, D. H.; Schniepp, H. C.; Chen, X.; Ruoff, R. S.; NGUYEN, S. T.; Aksay, I. A.; Prud'Homme, R. K.; Brinson, L. C. *Nature Nanotech* **2008**, *3* (6), 327.

(13) Kymakis, E.; Amaratunga, G. A. J. *Appl. Phys. Lett.* **2002**, *80* (1), 112.

(14) Liu, Q.; Liu, Z.; Zhang, X.; Zhang, N.; Yang, L. *Applied Physics …* **2008**.

(15) Liu, Z.; Liu, Q.; Huang, Y.; Ma, Y.; Yin, S.; Zhang, X.; Sun, W.; Chen, Y. *Adv. Mater.* **2008**, *20* (20), 3924.

(16) Barpuzary, D.; Qureshi, M. In *Graphene-Based Polymer Nanocomposites in Electronics*; Sadasivuni, K. K., Ponnamma, D., Kim, J., Thomas, S., Eds.; Springer International Publishing: Cham, 2015; pp 157–191.

(17) Berson, S.; de Bettignies, R.; Bailly, S.; Guillerez, S.; Jousselme, B. *Adv. Funct. Mater.* **2007**, *17* (16), 3363.

(18) Cai, J.; Pignedoli, C. A.; Talirz, L.; Ruffieux, P.; Söde, H.; Liang, L.; Meunier, V.; Berger, R.; Li, R.; Feng, X.; Müllen, K.; Fasel, R. *Nature Nanotech* **2014**, *9* (11), 896.

(19) Lee, S. J.; Kim, J.-Y.; Kim, H. P.; Kim, D.; da Silva, W. J.; Schneider, F. K.; bin Mohd Yusoff, A. R.; Jang, J. *Chem. Commun. (Camb.)* **2015**, *51* (44), 9185.

2 Synthesis and Characterization of Nitrogen Doped Chevron Graphene Nanoribbons

2.1 Introduction

Although the properties of graphene nanoribbons have been the topic of theoretical studies since 2004, the synthesis has been discovered within the last decade.[1-3] In order to obtain ribbons of narrow widths, top-down or bottom-up approaches may be used. These include lithographic patterning of graphene, sonochemical breaking of chemically derived graphene, metal-catalyzed cutting of graphene, chemical vapor deposition, chemical synthesis, and unzipping of carbon nanotubes.[3]

Top-down syntheses usually rely on commercially available or highly accessible starting materials that are transformed to the desired material via an uncontrolled process. Therefore, edge definition and width control is difficult to obtain, usually leading to defects and lack of control over the electronic properties of the ribbons. The common top-down synthesis of graphene nanoribbons is the exfoliation of carbon nanotubes, accomplished by plasma etching or the oxidation of CNT by potassium permanganate. Both of these synthetic methods result in ribbons with defective CO, COOH, OH, and CHO edges.[4,5] On the other hand, bottom-up syntheses of GNRs provide atomic control over the edge structure, width, doping, and dispersibility of the ribbons. However, these syntheses usually require the chemical synthesis of monomers and may require several steps and purifications. In 2010, Cai et al. reported the first bottom-up synthesis of GNRs on an Au(111) surface.[6] Brominated precursors such as 10,10'-dibromo-9,9'-bianthryl and 6,11-dibromo-1,2,3,4-tetraphenyltriphenylene were vacuum deposited on a Au(111) surface, polymerizing them, and heating further to activate cyclodehydrogenation. These steps are depicted on Figure 1.

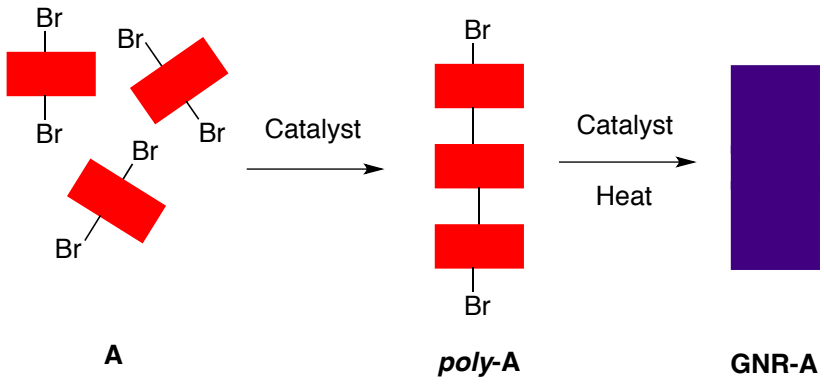

*Figure 1. Polymerization of precursor **A**, followed by cyclodehydrogenation leads to the formation of **GNR-A**.*

2.2 Synthesis of Nitrogen-Doped Graphene Nanoribbons

Recently, Vo et al. reported a solution-based synthesis of nitrogen-doped chevron GNRs.[7] In order to maximize charge transfer, it was imperative to use choose a GNR with a LUMO lower than that of the donor polymer. Therefore, GNR with 4 nitrogen atoms per monomer was chosen due to its high doping concentration and low LUMO (-3.9 eV). Figure 2 depicts the synthetic procedures carried out to synthesize this material.

Bromination of phenanthrene-9,10-dione, **1**, was performed with N-bromosuccinimide in sulfuric acid to obtain **2** in 53% yield. Condensation of **2** with 1,3-diphenylacetone was achieved by slow addition of potassium hydroxide in methanol, giving **2** in 67% yield. Diels-Alder of **3** with 1,2-di(pyrimidin-5-yl)ethyne in diphenyl ether yielded monomer precursor **4** in 48% yield. Polymerization of **4** with Bis(1,5-cyclooctadiene)nickel(0) to yield large molecular weight poly-**4** in 63% yield. Finally, Scholl oxidation with iron(III) chloride of poly-**4** yielded the desired nitrogen doped GNR-**4**.

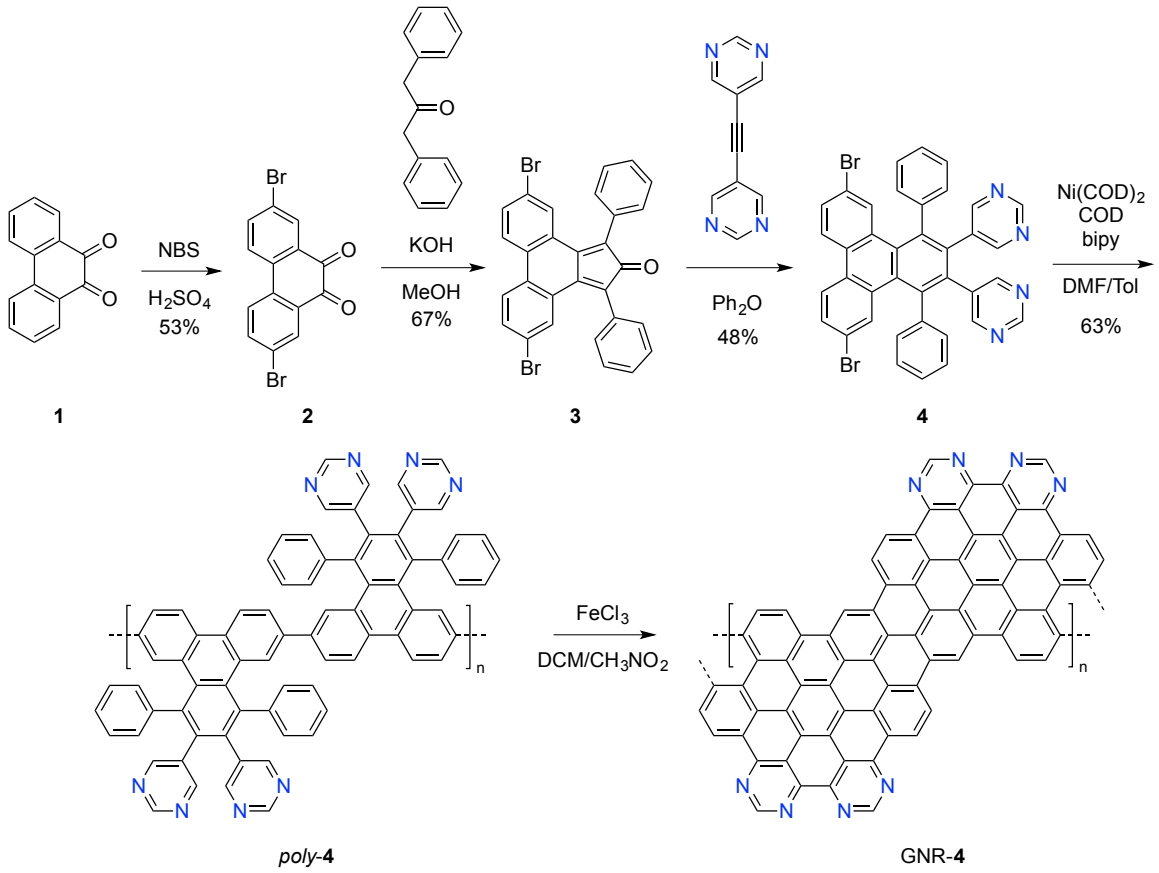

*Figure 2. Synthesis of GNR-**4** used as acceptor and transport pathway for OPVs in this work.*

2.3 Characterization of Nitrogen-Doped Graphene Nanoribbons

Characterization by proton nuclear magnetic resonance (^{1}H NMR), carbon nuclear magnetic resonance (^{13}C NMR), and matrix-assisted laser desorption/ionization (MALDI) confirmed the identity of all products except GNR-**4**. Due to aggregation, it is difficult to obtain solution-based characterizations of this material. Therefore, Raman spectroscopy was carried out to confirm its identity. The prominent G peak associated with monolayer graphene at ~1590 cm^{-1}, 2D at 2700 cm^{-1}, D+G mode at ~2950 cm^{-1}, and the intense D mode at ~1300 cm^{-1} commonly seen in graphene are present in the spectrum. The Raman spectrum of GNR-**4** also exhibits a width-specific radial breathing-like mode at ~400 cm^{-1}.[8]

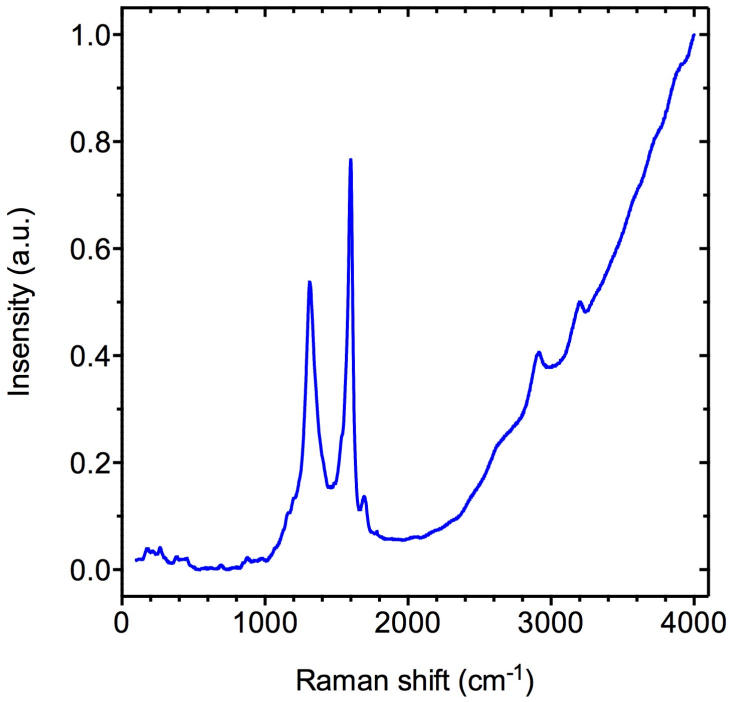

Figure 3. Raman spectrum of GNR-4 exhibiting the G, D, and D+G modes characteristic of GNRs.

Prior to fabricating devices, solubility tests were performed. GNR-**4** is dispersible in tetrahydrofuran (THF), and minimally so in chlorobenzene. The dispersiblity could not be improved by adding THF to dispersion of chlorobenzene, dichlorobenzene, toluene, and chloroform. Due to the high processability of chlorobenzene suspensions, chlorobenzene is the solvent of choice for most of the experiments reported in this work.

2.4 References

(1) Finkenstadt, D.; Pennington, G.; Mehl, M. J. *Phys. Rev. B* **2007**, *76* (12), 121405.

(2) Novoselov, K. S.; Geim, A. K.; Morozov, S. V.; Jiang, D.; Zhang, Y.; Dubonos, S. V.; Grigorieva, I. V.; Firsov, A. A. *Science* **2004**, *306* (5696), 666.

(3) Ma, L.; Wang, J.; Ding, F. *Chemphyschem* **2013**, *14* (1), 47.

(4) Jiao, L.; Zhang, L.; Wang, X.; Diankov, G.; Dai, H. *Nature* **2009**, *458* (7240), 877.

(5) Kosynkin, D. V.; Higginbotham, A. L.; Sinitskii, A.; Lomeda, J. R.; Dimiev, A.; Price, B. K.; Tour, J. M. *Nature* **2009**, *458* (7240), 872.

(6) Cai, J.; Ruffieux, P.; Jaafar, R.; Bieri, M.; Braun, T.; Blankenburg, S.; Muoth, M.; Seitsonen, A. P.; Saleh, M.; Feng, X.; Müllen, K.; Fasel, R. *Nature* **2010**, *466* (7305), 470.

(7) Vo, T. H.; Shekhirev, M.; Kunkel, D. A.; Orange, F.; Guinel, M. J. F.; Enders, A.; Sinitskii, A. *Chem. Commun.* **2014**, *50* (32), 4172.

(8) Cai, J.; Pignedoli, C. A.; Talirz, L.; Ruffieux, P.; Söde, H.; Liang, L.; Meunier, V.; Berger, R.; Li, R.; Feng, X.; Müllen, K.; Fasel, R. *Nature Nanotech* **2014**, *9* (11), 896.

3 Organic Photovoltaics Employing P3HT As The Donor and Graphene Nanoribbons

3.1 Introduction

In the field of polymer solar cell research, poly(3-hexylthiophene) (P3HT) remains the most commonly studied donor polymer. Graphitic materials may be employed in OPVs, but the processability of these materials need to be optimized. In 2011, Ren et al. reported the use of carbon nanotubes (CNT) as electron acceptors in a P3HT OPV. Record efficiency of 0.72% for a P3HT/CNT solar cell was achieved by aging the dispersion.

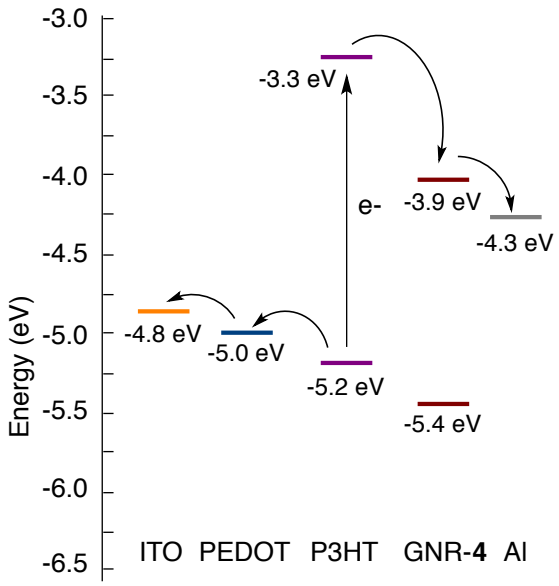

Figure 1. Energy levels of the HOMO and LUMO of the materials present in the OPV.

The performance of solar cells is highly variant on the optical properties of the polymer film. Ideally, the exciton dissociation is highly efficient in a solar cell. This process is dependent on the energy between the LUMO of the donor and the acceptor, ΔLUMO. Ideally, ΔLUMO is

greater than the Coulombic attraction of the electron and hole. The value for ΔLUMO should exceed 0.3 eV, which is a typical value for the exciton dissociation energy, leading to the separation of the geminate pair.[1] According to Cai et al. the band gap of GNR-**4** is in the order of 1.5 eV with the LUMO situated at -3.9 eV and the HOMO situated at -5.4 eV.[2] These values correspond to a ΔLUMO between P3HT and GNR-**4** of 0.6 eV, above the Coulombic attraction energy. P3HT was investigated in this work due to its energy level position relative to that of the synthesized GNR-**4** and its widely studied properties (Figure 1). Herein we report the characterization of P3HT/GNR films and their use as the photoactive layer in OPV devices.

3.2 Absorption and Emission of P3HT/GNR Films

Exciton dissociation from donor to acceptor could be monitored by fluorescence spectroscopy. Addition of an efficient electron acceptor would significantly quench the photoluminescence of the donor. The absorption and emission spectrum of P3HT film deposited from 10 mg/mL in chlorobenzene was obtained (Figure 2). The absorption and fluorescence of pristine P3HT films is shown in blue, and those of P3HT/GNR-4 is shown in red. Dashed lines correspond to the photoluminescence and solid lines to the absorption.

Similarly to other graphitic materials, the presence of GNR-**4** decreased the absorption of the film at concentrations of 28-55%.[1] This decrease in absorption, which is also observed in PCBM blends, tends to occur at lower concentrations than that of PCBM. Such a decrease in absorption may also be due to the scattering of light by the nanoribbons.[3] No considerable photoluminescence quenching is observed at this loading of nanoribbon in a 10:1 donor/acceptor blend. This finding supports the notion that charge transfer is not efficient. Counterintuitive to what was expected, a large expected ΔLUMO did not result in significant photoluminescence quenching. Two possible explanations for such discrepancy are 1) microaggregates of graphene

nanoribbons which minimize donor/acceptor interface area, and 2) aggregation of graphene nanoribbons shifts the LUMO level such that ΔLUMO is not favorable.

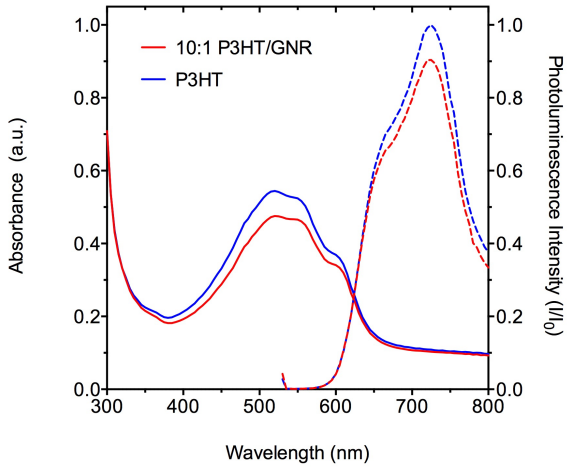

*Figure 2. Absorption (–) and emission (---) of P3HT in a pristine film, and in the presence of GNR-**4**. Fluorescence was measured with an excitation wavelength of 500 nm.*

In order to differentiate between the effects of donor/acceptor interface concentration and ΔLUMO, absorption and fluorescence of P3HT films with PCBM and GNR-**4** at different acceptor loading was obtained. Additionally, we ought to investigate the difference between a widely known efficient acceptor and our new material. The absorption and photoluminescence quenching of both acceptors normalized to the fluorescence of a pristine P3HT film is shown in Figure 3. While an increase in loading of PCBM has minimal effect in the absorption of P3HT film at 505 nm, the presence of the GNR significantly decreases the absorption of the film. At higher loadings, both GNR-**4** and PCBM productively quench the fluorescence of P3HT at 725 nm, excited at 500 nm. However, photoluminescence quenching by PCBM is achieved at donor to acceptor ratios as low as 1:0.4 while such effects is not observed with GNR-**4** even at ratio of 1:1.2. If the fluorescence were to be normalized to the absorbance, there would still be emission quenching by GNR-**4**, though smaller than PCBM. A probable reason for this difference would be

the aggregation of nanoribbons, resulting in a lower "effective" concentration, that is, lowers density of donor/acceptor interfaces, while PCBM effectively intercalates itself within the polymer matrix. The nanoscale phase separation in donor/acceptor materials must be smaller than the exciton diffusion length, which is generally less than 10 nm, otherwise recombination occurs. In conclusion, although PL quenching by the GNR is not as efficient as PCBM, the presence of charge transfer is supported by our data.

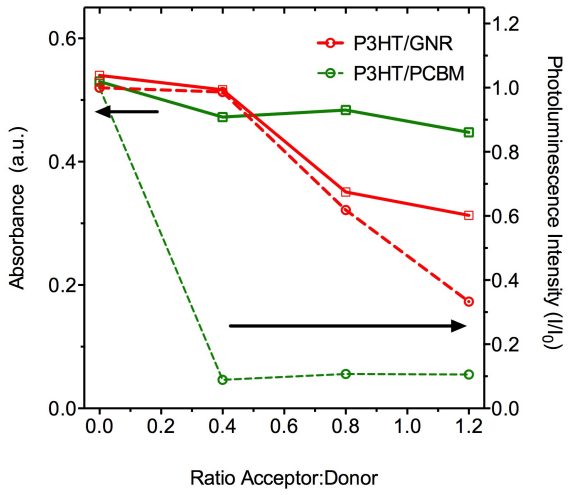

*Figure 3. Absorption (–) and emission (---) of P3HT films in the presence of GNR-**4** and PCBM.*

3.3 Graphene Nanoribbons as Electron Acceptors

Although photoluminescence quenching by GNR is not as efficient as PCBM, fluorescence data suggests that charge transfer still occurs. Due to the low solubility of graphene nanoribbons, it was pertinent to find the right solvent for active layer deposition. GNR-**4** contains 4 nitrogen units per monomer in the ribbon. This makes the GNRs ideal for dispersion in acidic water and polar solvents. However, such solvents are not ideal for OPV fabrication because they result in low yields and reproducibility due to their low boiling point or introduction of water into the cell. Solubility tests elucidated that the material is most dispersible in THF, followed by

chlorobenzene. Devices deposited from 10 mg/mL P3HT in THF or chlorobenzene with 10% GNR-**4** were studied. The device architecture is depicted in Figure 4, with indium tin oxide (ITO) as the anode, poly(3,4-ethylenedioxythiophene) polystyrene sulfonate (PEDOT:PSS) as the hole transport layer, P3HT/GNR as the active layer, and aluminum as the cathode.

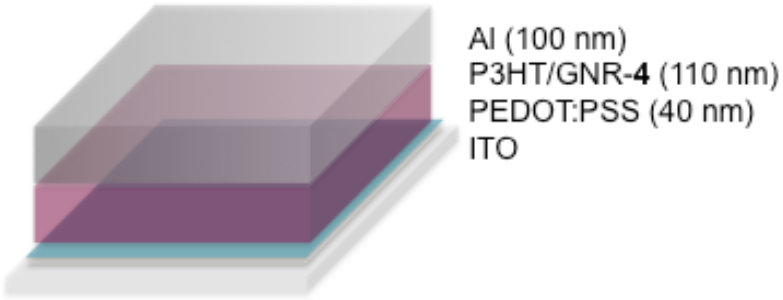

Figure 4. Device architecture of P3HT/GNR solar cells.

Figure 5 shows the most representative I-V curves of these OPVs. Although the THF OPVs gave greater Voc, their Jsc was smaller and the yield was low. This is likely due to the low boiling point of THF, resulting in films with nonuniform thicknesses. Pristine P3HT devices tend to posses leakage pathways and several were shorted. The devices fabricated from chlorobenzene solutions of P3HT/GNR-**4** perform better than pristine devices.

Table 1 summarizes the figures of merit for these devices. Perhaps the most notable characteristic of the GNR-**4** devices deposited from chlorobenze is their lower shunt resistance. Such finding supports the hypothesis that microdomains of nanoribbons exist in the cell, acting as a leakage pathway. On the other hand, devices deposited from THF possess a larger shunt resistance, due to the relatively high dispersion of the ribbons in the solvent. Higher loading of ribbon results in lower series resistance in both devices fabricated from chlorobenzene and THF solutions. Thus far, our data suggests that the ribbons do provide conducting pathways for free

charge carriers, both in productive and detrimental ways. However, such properties may be exploited, discussed in later sections of this chapter and in Chapter 4.

Although larger loadings of ribbons result in lower efficiencies for the cells constructed from chlorobenzene solutions, such a change improves the PCE of those fabricated from THF solutions. This is another finding that supports our hypothesis that aggregation is present in chlorobenzene devices, making it crucial to find a reliable solvent system for better OPVs. Overall, chlorobenzene was the solvent of choice due to its reliability, higher J_{sc}, lower R_s, and its record with P3HT.[4,5]

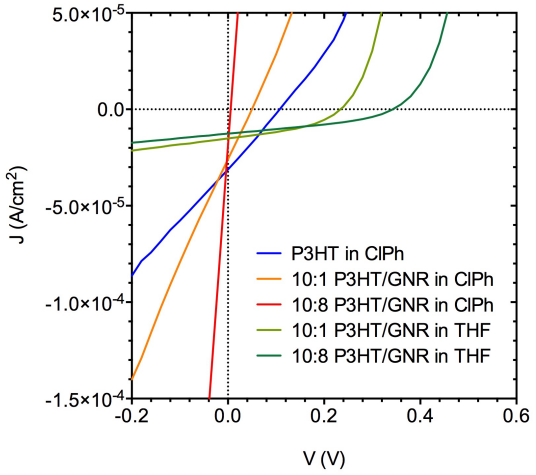

Figure 5. Representative I-V curves of P3HT/GNR solar cells deposited from chlorobenzene (ClPh) and from THF.

*Table 1. Figures of merit of P3HT/GNR-**4** OPVs*

Active Layer	Voc (V)	Jsc (A/cm^2)	FF	PCE	R_s (Ω•cm^2)	R_{sh} (Ω•cm^2)
P3HT	0.11	-3.11E-05	0.26	0.00087	123.04	26315.10
10:1 ClPh	0.05	-2.59E-05	0.25	0.00033	64.65	8692.87
10:8 ClPh	0.01	-1.92E-05	0.28	0.00003	42.33	332.29

10:1 THF	0.23	-1.51E-05	0.41	0.00143	366.42	427866.06
10:8 THF	0.34	-1.26E-05	0.37	0.00161	276.88	441505.02
10:1 ClPh Aged	0.51	-4.07E-05	0.31	0.00643	110.88	181022.49

Similar to previous studies using graphitic materials as conductive pathways, we studied the effect of GNRs in P3HT/PCBM OPVs. Using GNR-**4** as an additive for electron transfer in an OPV with an active layer of 10:8:1 P3HT/PCBM/GNR resulted in poor performance and a decrease in all parameters, except a similar fill factor and a lower series resistance. This is likely caused by the introduction of defect sites.

3.4 Improvement in Cell Performance by Aging Solutions

Films of P3HT have been known to have aggregated and crystalline domains.[6,7] Taking advantage of this property, Ren et al. reported that aging a solution of P3HT/CNTs with cyclohexanone overnight resulted in a uniform film.[8] The study claims that the presence of cyclohexanone leads to a micelle-like formation of nanofilaments containing carbon nanotubes in the center surrounded by P3HT chains. We ought to test whether such aging process would improve the film morphology and the performance of our photovoltaic devices. Solutions of 10:1 P3HT/GNR, 10 mg/mL in chlorobenzene were slowly mixed with cyclohexanone by volume. These solutions were left undisturbed overnight and filtered the next day to spin coat the glass substrates. The film absorptions were measured and compared to films deposited from THF and chlorobenzene without aging. The spectra show the characteristic inter-chain transitions $A_{0\text{-}0}$ (600-610 nm) and $A_{0\text{-}1}$(555 nm). Blue shift of the $A_{0\text{-}0}$ transition in the THF film suggests a lower concentration of crystallites in the film.[9] As expected, less order decreases the conjugation of the polymer chain leading to higher band gaps, and lower wavelengths. Additionally, the ratio of the amplitudes of $A_{0\text{-}0}$ and $A_{0\text{-}1}$ is largest for the film deposited from aged chlorobenzene solution

(0.72) and smallest for the one deposited from THF (0.65). The larger ratio of these amplitudes corresponds to more crystalline domains, and such values are characteristic of coexisting partially ordered aggregated and non-aggregated P3HT chains. The red shift and 0-0/0-1 ratio of the film deposited from the aged solution suggest an enhanced structural coherence length and intrachain order.[10] Finally, the addition of GNR-**4** to P3HT results in larger 0-0/0-1 ratios independent of solvent system. This suggests that the ribbons may provide some ordered structure, potentially through seeding via π-π stacking of P3HT with the ribbon. High order may decrease the amount of defects, and in the case of P3HT, increases the efficiency of the OPVs.[11]

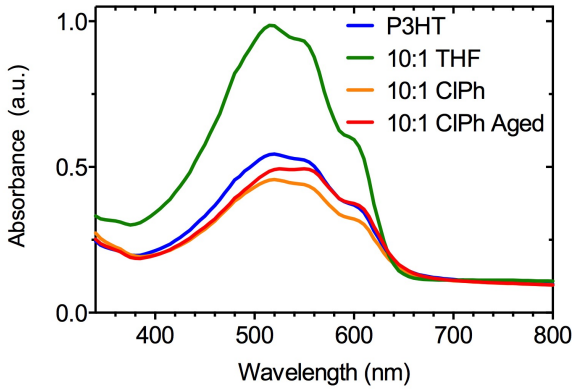

Figure 7. Film absorption of P3HT with GNR-4 from various solvent systems.

These films were investigated by Atomic Force Microscopy (AFM). As expected, the AFM images suggest a larger uniformity for the films deposited from aged solutions (Figure 8) as seen by a decrease of ~500 nm aggregates present in nonaged solutions (right, Figure 8). Additionally, surface roughness is increased from -8.9-17.8 nm (right) to -38.5-45.5 nm (left). Both of these effects would improve the performance of the OPV.

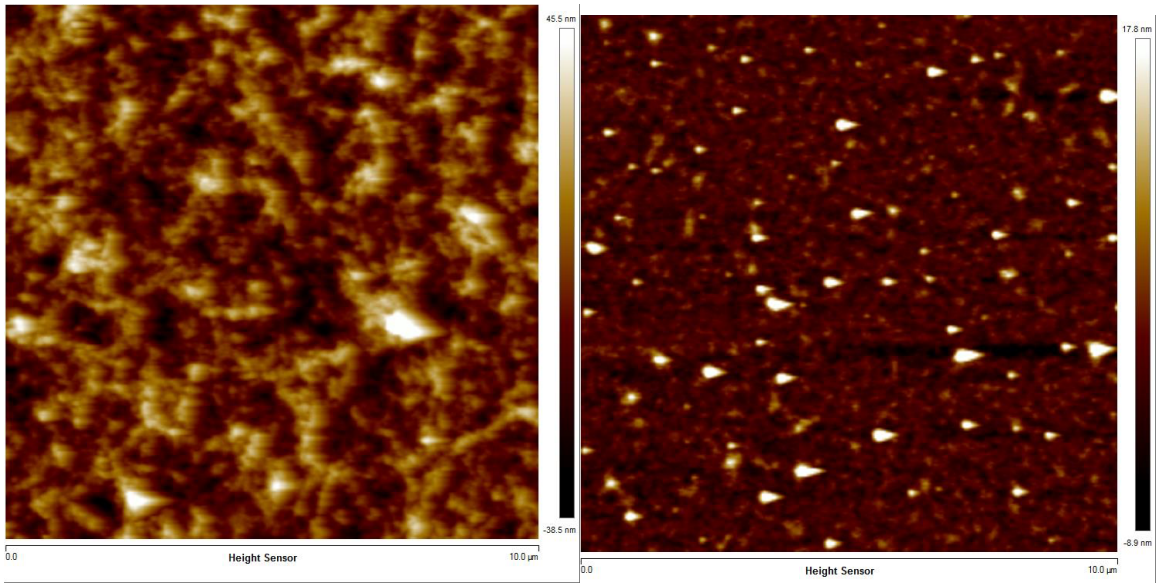

Figure 8. AFM of films deposited from aged (left) and not aged (right) solutions of 10:1 P3HT/GNR-4 in chlorobenzene. The images are 10x10 µm and the height is -38.5-45.5 nm (left) and -8.9-17.8 nm (right)

Devices fabricated from aged solutions exhibited superior performance. Figure 9 summarizes the results. Aging results in a significant improvement on most figures of merit, specifically a ten-fold improvement in V_{oc}, 60% increase in J_{sc}, twenty fold increase in PCE, and increase in shunt resistance (Table 1). Aging is required to ensure maximum integration of GNR-**4** into the donor polymer matrix. Although aging improves the performance of the solar cell, the figures of merit of these solar cells remain behind current P3HT solar cells that have a PCE of 5%.[11] Aggregation of the ribbons result in low intercalation of the GNR within the P3HT film.

An attempt to study the effect of GNR loading was carried out. An increase in loading results high leakage current, and no change in V_{oc}, J_{sc}, FF, and PCE is observed by varying the loading of acceptor. This observation supports the notion that the amount of GNR that interfaces with the donor is saturated even at the small loadings of 10:0.05 P3HT/GNR. Additionally, the leakage current likely occurs by microdomain GNR aggregates being in direct contact with the cathode and anode.

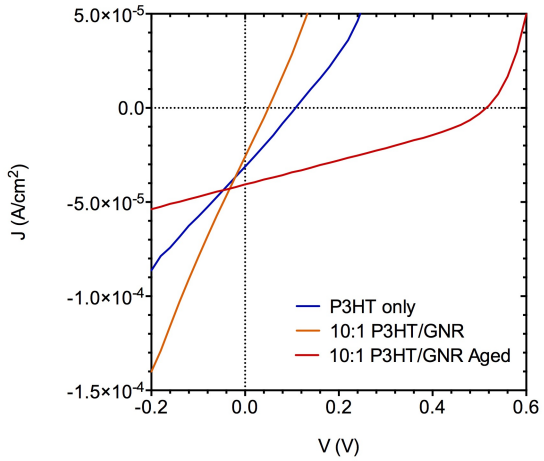

Figure 9. I-V characteristic of devices fabricated with aged P3HT/GNR solutions.

3.5 Conclusions and Outlook

Graphene nanoribbons have many properties that make them ideal candidates for OPVs, including high mobility, high thermal and atmospheric stability, and high tensile strength. Their ability to have strong π-π interactions may result in strong donor/acceptor interactions, but also in detrimental aggregation. In this study, we observed that inclusion of GNR-**4** in a polymer cell decreases the series resistance by providing conductive pathways, as well as increase the order of the film. However, for GNR-4 to be a liable acceptor for P3HT films, it is pertinent to increase their dispersibility by identifying new solvents or alkylating the nitrogen with long chains.

3.6 References

(1) Ratier, B.; Nunzi, J. M.; Aldissi, M.; Kraft, T. M. *Polymer* **2012**.

(2) Cai, J.; Pignedoli, C. A.; Talirz, L.; Ruffieux, P.; Söde, H.; Liang, L.; Meunier, V.; Berger, R.; Li, R.; Feng, X.; Müllen, K.; Fasel, R. *Nature Nanotech* **2014**, *9* (11), 896.

(3) Bonaccorso, F.; Sun, Z.; Hasan, T.; Ferrari, A. C. *Nature Photon* **2010**, *4* (9), 611.

(4) Kim, J. Y.; Lee, K.; Coates, N. E.; Moses, D.; Nguyen, T.-Q.; Dante, M.; Heeger, A. J. *Science* **2007**, *317* (5835), 222.

(5) Machui, F.; Langner, S.; Zhu, X.; Abbott, S.; Brabec, C. J. *Solar Energy Materials and Solar Cells* **2012**, *100*, 138.

(6) Berson, S.; de Bettignies, R.; Bailly, S.; Guillerez, S.; Jousselme, B. *Adv. Funct. Mater.* **2007**, *17* (16), 3363.

(7) Rahimi, K.; Botiz, I.; Agumba, J. O.; Motamen, S.; Stingelin, N.; Reiter, G. *RSC Advances* **2014**, *4* (22), 11121.

(8) Ren, S.; Bernardi, M.; Lunt, R. R.; Bulovic, V.; Grossman, J. C.; Gradecak, S. *Nano Lett.* **2011**, *11* (12), 5316.

(9) Clark, J.; Silva, C.; Friend, R. H.; Spano, F. C. *Phys. Rev. Lett.* **2007**, *98* (20), 206406.

(10) Baghgar, M.; Labastide, J.; Bokel, F.; Dujovne, I.; McKenna, A.; Barnes, A. M.; Pentzer, E.; Emrick, T.; Hayward, R.; Barnes, M. D. *J. Phys. Chem. Lett.* **2012**, *3* (12), 1674.

(11) Ma, W.; Yang, C.; Gong, X.; Lee, K.; Heeger, A. J. *Adv. Funct. Mater.* **2005**, *15* (10), 1617.

4 Organic Photovoltaics Employing PCDTBT As The Donor and Graphene Nanoribbons As Electron Transport Pathways

4.1 Introduction

While P3HT films may contain crystalline domains, other donor polymers tend to exhibit an amorphous morphology. One might expect that changing the film morphology of the donor may have a large impact on the performance of solar cells fabricated with materials that are challenging to disperse, such as GNRs. One such polymer is *poly*[*N*-900-hepta-decanyl-2,7-carbazole-alt-5,5-(40,70-di-2-thienyl-20,10,30-benzothiadiazole)] (PCDTBT).[1] PCDTBT is known to have an internal quantum efficiency of nearly 100%, good thermal stability, and long lifetimes of nearly 7 years.[1] To our knowledge there is only one report of the use of graphitic materials in the active layer of a PCDTBT OPV. Gusain et al. reported at a conference an improvement in PCE of 30% and in J_{sc} of 37% by incorporating graphene sheets in the hole transport layer of a PCDTBT/$PC_{71}BM$ OPV.[2] Furthermore, addition of graphene sheets to a P3HT/$PC_{71}BM$ OPV results in a two-fold increase in efficiency by modifying the HOMO and the LUMO of $PC_{71}BM$ through π-π stacking and providing an efficient electron transport pathway.[3] Based on the energy levels of the GNR-**4**, the ribbon may provide a pathway for either electron or holes (Figure 1). However, it is expected that the GNR would mostly interface with the fullerene due to better interaction and higher concentrations in a 10:37 PCDTBT/PC71BM OPV.

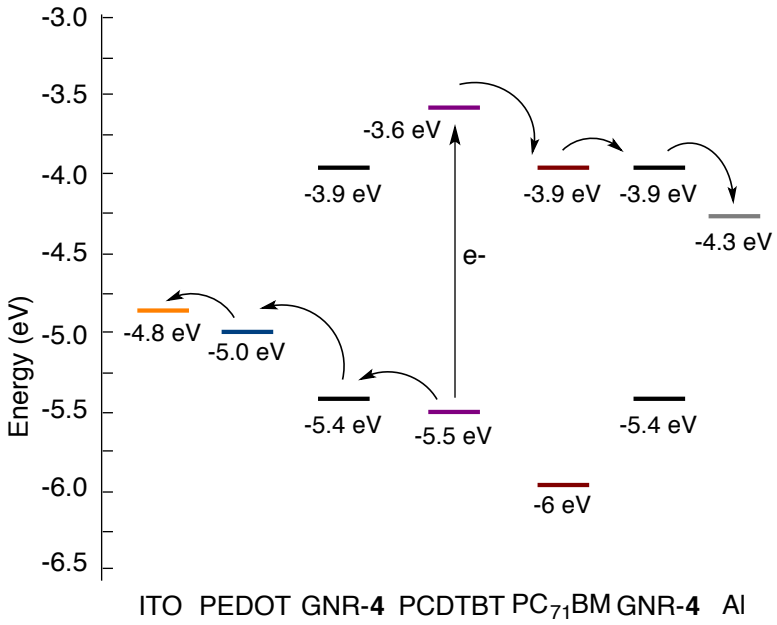

Figure 1. Energy levels of the HOMO and LUMO of the materials present in the OPV fabricated.

4.2 Optical Properties of PCDTBT/GNR Films

Similar to what we observed with P3HT, addition of GNRs into PCDTBT films did not have much effect in the amplitude of absorbance and emission of PCDTBT. This supports the notion that charge transfer is not efficient between PCDTBT and the ribbon. However, a red shift of ~5 nm suggests an increase in planarity of the donor chains, as observed with P3HT.

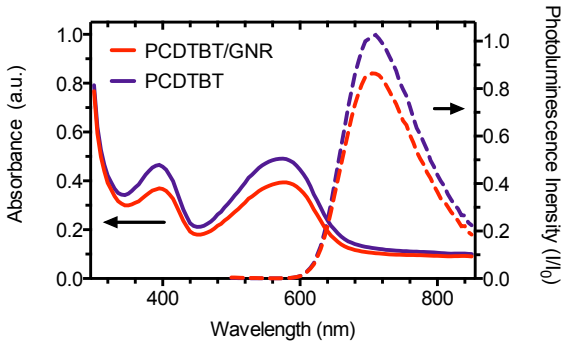

*Figure 2. Absorption (−) and emission (---) of P3HT in a pristine film, and in the presence of GNR-**4**. Fluorescence was measured with an excitation wavelength of 500 nm.*

4.3 Organic Photovoltaics Using GNR as Electron Transport Pathway

The device architecture is depicted in Figure 3, with indium tin oxide (ITO) as the anode, poly(3,4-ethylenedioxythiophene) polystyrene sulfonate (PEDOT:PSS) as the hole transport layer, PCDTBT/PC71BM/GNR as the active layer, and aluminum as the cathode. In order to comprehend the effect of GNR-**4** on cell performance, three controls were fabricated. The controls had active layers containing 1) PCDTBT only, 2) PCDTBT/GNR, and 3) PCDTBT/PC71BM.

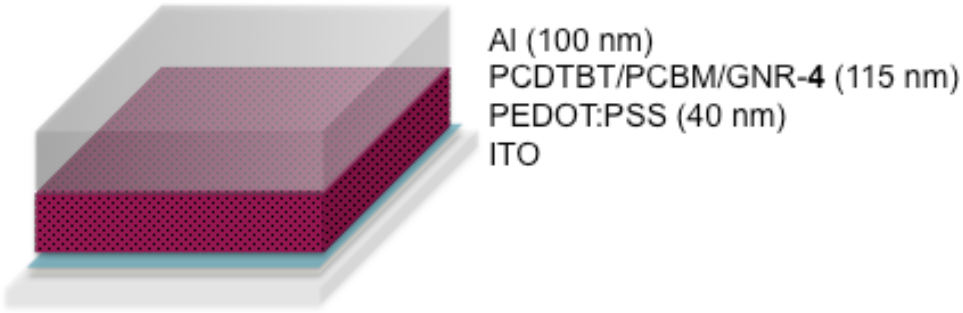

Figure 4. Device architecture of PCDTBT/PC71BM/GNR solar cells.

The most representative I-V curves of these OPVs are shown in Figure 5, and the figures of merit are summarized in Table 1. A significant improvement in cell performance is observed when GNR-**4** is added to the active layer in a 10:37:1 PCDTBT/PC71BM/GNR ratio. The PCE increases by 18% and the J_{sc} by 15%. This improvement is likely not caused by the ribbon acting as acceptor, since devices fabricated with GNR as the acceptor showed no photovoltaic performance improvement over the PCDTBT OPV control. Additionally, the series and shunt resistance decrease in light. Perhaps, a more descriptive comparison would be that of the shunt and series resistance in the dark. The series and shunt resistance in the dark for the PCDTBT/PC71BM OPV were 161 ($\Omega \bullet cm^2$) and 23,137,276 ($\Omega \bullet cm^2$), respectively. On the other hand, the series and shunt resistance in the dark for the PCDTBT/PC71BM/GNR OPV were 121 ($\Omega \bullet cm^2$) and 38,577,419 ($\Omega \bullet cm^2$), respectively. This is in agreement with the notion that the ribbons are anisotropic and they provide conductive pathways for free charges. However, the increase in shunt resistance may be due to the prevention of aluminum "spikes" by effectively dissipating heat during evaporation.

Considering an ohmic contact between the electrodes and the cell, the V_{oc} may be described as $V_{oc} = (1/e)\ (|HOMO^{donor}| - |LUMO^{acceptor}|) - V$, where $0.2\ V < V < 0.5$ eV depending on the material and its properties. [4] Because the V_{oc} remains almost constant, one may assume that the LUMO of the fullerene is not significantly impacted by the presence of the ribbon, in contrast with the report by Chauhan et al. for their P3HT/PC71BM/Graphene device.[3] This is likely due to the difference in surface area between graphene nanoribbons and graphene sheets. One may question whether this effect is caused by the small loading of GNR to PC71M in our devices. However, Chauvin et al. device contains even smaller ratios of 34:37:0.0185 P3HT/PC71BM/Graphene compared to this study (10:37:1 PCDTBT/PC71BM/GNR).

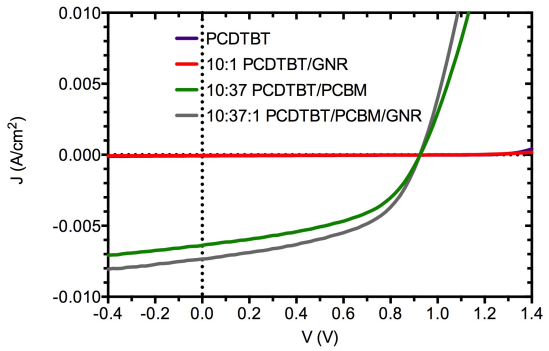

Figure 5. Representative I-V curves of PCDTBT/PC71BM/GNR solar cells.

Using graphene nanoribbons as acceptors proved to be counterproductive in a PCDTBT active layer. One may conclude that this may be due to the large loading of acceptor usually required for high performing PCDTBT solar cells not present in the reported cell herein. Solar cells with larger amounts of GNR-**4** were fabricated, mostly resulting in leaky OPVs.

Table 1. Figures of merit of PCDTBT OPVs

Active Layer	Voc (V)	Jsc (A/cm^2)	FF	PCE	R_s (Ω•cm^2)	R_{sh} (Ω•cm^2)
PCDTBT	1.19	-7.52E-05	0.26	0.02	1572.57	111965.16
10:1 PCDTBT/GNR	1.11	-5.00E-05	0.27	0.015	17382.55	199860.10
10:37 PCDTBT/PC71BM	0.93	-6.37E-03	0.49	2.88	145.19	14784.20
10:37:1 PCDTBT/PC71BM/GNR	0.92	-7.34E-03	0.50	3.41	119.34	10372.00

4.4 Conclusion and Outlook

The amorphous morphology of PCDTBT requires high amounts of PC71BM to ensure optimal donor/acceptor network.[5] The addition of merely 2% of GNR-**4** provides a conductive pathways for electrons to reach the cathode. This effect is observed in the decrease in series

resistance, improvement of J_{sc} to -7.34 mA/cm^2, and an increase in PCE to 3.41%. It is pertinent to attempt various loadings of GNRs to optimize the ratio of PCDTBT/PC71BM/GNR. Furthermore, cyclic voltammetry of PC71BM, GNR, and PC71BM/GNR could elucidate the effect of GNR on the LUMO of the fullerene. Finally, employing GNR-**4** as a hole transport layer may clarify the role of the GNR in the OPV. This work has shown that graphene nanoribbons are potential materials for the new wave of OPVs.

4.5 References

(1) Beaupré, S.; Leclerc, M. *Journal of Materials Chemistry A* **2013**, *1* (37), 11097.

(2) Gusain, A.; Chauhan, A. K.; Jha, P.; Koiry, S. P.; Veerender, P.; Saxena, V.; Varde, P. V.; Aswal, D. K.; Gupta, S. K. *... : Proceedings of the ...* **2015**, *1665* (1), 050122.

(3) Chauhan, A. K.; Gusain, A.; Jha, P.; Koiry, S. P.; Saxena, V.; Veerender, P.; Aswal, D. K.; Gupta, S. K. *Appl. Phys. Lett.* **2014**, *104* (13), 133901.

(4) Ratier, B.; Nunzi, J. M.; Aldissi, M.; Kraft, T. M. *Polymer* **2012**.

(5) Park, S. H.; Roy, A.; Beaupré, S.; Cho, S.; Coates, N.; Moon, J. S.; Moses, D.; Leclerc, M.; Lee, K.; Heeger, A. J. *Nature Photon* **2009**, *3* (5), 297.